Molecular BioSystems

Accepted Manuscript

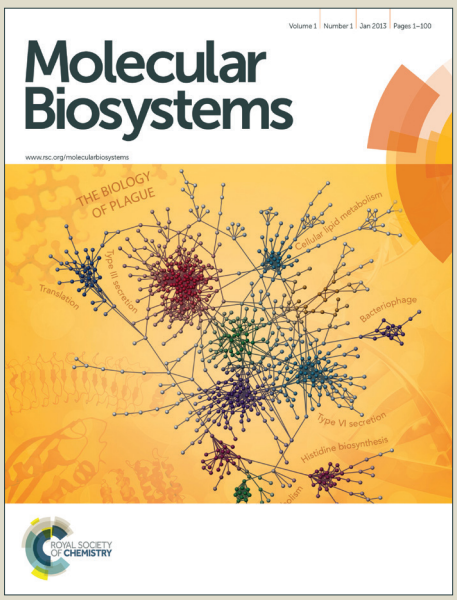

ROYAL SOCIETY OF CHEMISTRY

www.rsc.org/molecularbiosystems

Graphical abstract

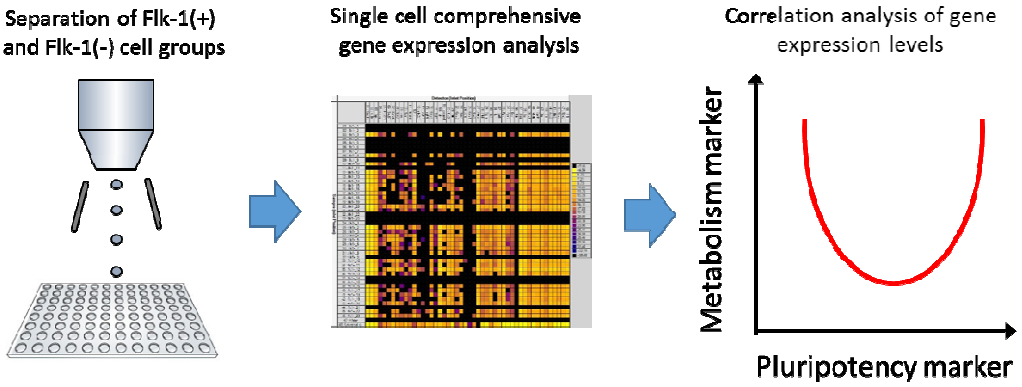

Metabolic suppression has been revealed during mesodermal differentiation by using single-cell gene expression analysis.

Molecular BioSystems

ARTICLE

Metabolic suppression during mesodermal differentiation of embryonic stem cells identified by single-cell comprehensive gene expression analysis

Received 00th January 20xx,
Accepted 00th January 20xx

DOI: 10.1039/x0xx00000x

www.rsc.org/

Yuanshu Zhou,[a] Ikuma Fujisawa,[b] Kosuke Ino,[b] Tomokazu Matsue[ab] and Hitoshi Shiku[*b]

Flk-1 (VEGF receptor 2) is a well-defined mesodermal progenitor marker and the Flk-1-positive (Flk-1(+)) cells derived from embryonic stem cells (ESCs) have been known to generate hemangioblasts and cardiovascular progenitor cells, which are formed in the early and late stages of differentiation, respectively. In this study, we separated Flk-1(+) and Flk-1(-) cells from spontaneously differentiating embryoid bodies (EBs) of mouse ESCs. We found cell aggregates derived from late stage Flk-1(+) cells had a relatively small size and low oxygen consumption rate (OCR) compared with those derived from Flk-1(-) cells. Furthermore, using single-cell comprehensive gene expression analysis, we found that both Flk-1(+) and Flk-1(-) cells could be categorized into subgroups with either low or high glucose metabolic activity. We observed that metabolic suppression occurs in cells expressing an intermediate level of both *Nanog* and *Pou5f1*. Taken together, our data suggested the temporary metabolic suppression is an intrinsic feature of mesodermal differentiation.

1. Introduction

Embryonic stem cell (ESC)-derived heart-contributing cells hold great promise for regenerative medicine and organ transplantation.[1, 2] Nevertheless, prior to generate functional mature cardiomyocytes, ESCs underwent a moderate differentiation stage called mesodermal progenitor cells. Fluorescence-activated cell sorting (FACS) analysis has made a breakthrough in the process of obtaining purified mesodermal progenitor cells free of remaining undifferentiated cells when combined with a well-defined surface marker, Flk-1 (VEGF receptor 2; Kdr).[3-6] Notably, the timing of FACS sorting for spontaneously differentiating cells is commonly highlighted in these studies. Kattman et al.[7] used the mouse ESC differentiation model to demonstrate that Flk-1(+) cells formed in the early and late stages are mainly used to generate hemangioblasts and cardiovascular progenitor cells, respectively. Zhang et al.[8] reported that Flk-1(+) cells can be further separated into different definitive mesodermal lineages with the combination of another surface marker, podocalyxin. However, these findings focused mainly on the difference of differentiation level.

Because of the hypoxic environment prior to implantation, ESCs derived from the inner cell mass of the mammalian embryo rely mainly on glycolysis to produce energy.[9] In addition, hypoxia has been found to increase the percentage of Flk-1(+) mesodermal progenitor cells.[10] Interestingly, the effects of hypoxia on cardiac differentiation are diverse. Chronic hypoxia has been previously shown to give rise to apoptosis in fetal rat heart, [11] whereas transient hypoxia in an appropriate period exerts a positive role on cardiomyocyte differentiation in mouse ESCs.[12] On the other hand, although oxidative phosphorylation and oxygen consumption is necessary for cardiomyocyte contraction, [13] a lactate medium without glucose found to be extremely effective for the purification of mature cardiomyocytes.[14] These studies suggested that metabolic activity is changed dynamically in the process of mesodermal differentiation.

Using a mouse ESC-derived spontaneously differentiating embryoid body (EB) model, we have previously evaluated the oxygen consumption rate (OCR) of individual EBs and found the expression of differentiation-related genes to be positively correlated with the OCR level, regardless of the direction of differentiation.[15] In this study, we separated Flk-1(+) cells at different time points of differentiation and cultured them as 3D cell aggregates. As a result, we found that cell aggregates derived from the late stage Flk-1(+) cells had a lower growth potential and OCR levels than those derived from Flk-1(-) cells. Furthermore, by using Fluidigm's multiplex PCR-based Biomark HD system, we compared comprehensive gene expression profiles of late stage Flk-1(+) cells and Flk-1(-) cells on single-cell level. We succeeded in separating the Flk-1(+) and Flk-1(-) cells into subgroups with low/high metabolic activity on the basis of the expression of genes encoding crucial glucose metabolic enzymes. Flk-1(+) cells showed reduced metabolic activity also expressed an intermediate level of pluripotency markers *Nanog* and *Pou5f1*, suggested that temporary metabolic suppression is an intrinsic feature of mesodermal differentiation. Our study provides new insight into the metabolic regulation that occurs during tissue development.

[a] WPI-Advanced Institute for Materials Research, Tohoku University, Sendai 980-8577, Japan
[b] Graduate School of Environmental Studies, Tohoku University, 6-6-11-604 Aramaki-Aoba, Sendai 980-8579, Japan

2. Materials and methods

Embryonic stem cell culture and embryoid body differentiation

A mouse ES cell line (strain 129/SVE) was purchased from DS Pharma Biomedical Co., Ltd. The cells in their undifferentiated state were maintained in StemMedium serum-free media (DS Pharma Biomedical Co., Ltd.), containing 1000 U mL^{-1} leukemia inhibitory factor, 1% penicillin/streptomycin, and 0.1 mM β-mercaptoethanol, in 0.1% gelatin-coated flasks. The cells were incubated at 37 °C under a 5% CO_2 atmosphere. The medium was replaced every day. Spontaneous differentiation of the ESCs was induced by forming EBs. EBs formed by hanging drop were cultured in StemMedium containing 15% fetal bovine serum (FBS), 1% penicillin/streptomycin, and 0.1 mM β-mercaptoethanol (1000 cells per 20-μL drop of medium). EBs formed in 35-mm petri dishes were cultured in Iscove's Modified Dulbecco's Medium (IMDM; Sigma) containing 15% FBS, 1% penicillin/streptomycin, 2 mM L-glutamine (Life Technologies), 0.5 mM ascorbic acid (Sigma), and 4.5×10^{-4} M monothioglycerol (MTG; Sigma).

Flow cytometry and re-aggregation

The EBs were harvested and treated with Spheroid Dispersion Solution (SD4X; SCIVAX), single-cell suspensions were analyzed or sorted on a MoFlo XDP flow cytometer (Beckman Coulter). Cells were stained by using a PE-conjugated anti-Flk-1 mAb (R&D Systems). Dead cells, which were identified by 7-AAD Viability Dyes solution staining (Beckman Coulter), were excluded from the analysis. Data were recorded with the Summit software donated by Beckman Coulter. For re-aggregation of cells separated from EBs formed by hanging drop, 1000 sorted cells were collected in 100 μL of StemMedium (containing 15% FBS, 1% penicillin/streptomycin, and 0.1 mM β-mercaptoethanol) per well in PrimeSurface 96-well U-bottom plates (Sumitomo Bakelite). For re-aggregation of cells separated from EBs formed in petri dishes, 1000 sorted cells were collected in 100 μL of IMDM (containing 15% FBS, 1% penicillin/streptomycin, 2 mM L-glutamine, 0.5 mM ascorbic acid, 4.5×10^{-4} M MTG, 5 ng mL^{-1} mVEGF (Wako), and 30 ng mL^{-1} hbFGF (Sigma)) per well in PrimeSurface 96-well U-bottom plates.

OCR measurement

Oxygen consumption rate (OCR) measurement of cell aggregates was performed as previously described.[16, 17] In brief, samples were transferred individually into appropriate plates (Research Institute for the Functional Peptides, Yamagata, Japan) filled with 3 mL of Embryo Respiration Assay Medium 2 (Research Institute for the Functional Peptides), by using a mouth pipette. Oxygen reduction currents were monitored using a 10-μm-radius Pt disk microelectrode probe at -0.5 V versus Ag/AgCl. The electrode probe was scanned vertically from the side of the cell aggregate up to 160 μm. This up and down movement was repeated six times by using a commercially available scanning electrochemical microscope system (HV405; Hokuto Denko). The OCR level of the cell aggregate (F, in units of mol s^{-1}) was obtained according to the spherical diffusion equation:

$$F = \frac{D}{0.7} \times 2\pi \left(1 - \frac{1}{\sqrt{2}}\right)\left(1 + \sqrt{2}\right) R \Delta C \quad (1)$$

where ΔC (mol cm^{-3}) is the difference in oxygen concentration between the sample surface and the bulk solution, and D is the diffusion coefficient of oxygen (2.1×10^{-5} cm^2 s^{-1}). The mean sample radius (R, in unit of cm) of the cell aggregate was based on the microscope image and analyzed by ImageJ software.

Single-cell collection and STA

A total of 48 individual primer pair mixes were pooled to make a specific target amplification (STA) multiplex primer mix (Table S1). Each primer was at a final concentration of 200 nM. Single-cell reverse transcription and the STA reaction were carried out by using the CellsDirect One-Step qRT-PCR Kit (Invitrogen) according to the manufacturer's manual. In brief, individual cells were sorted directly into PCR tubes loaded with 5 μL of CellsDirect 2X Reaction Mix, 0.2 μL of SuperScript III RT Platinum Taq Mix, 2.5 μL of STA multiplex primer mix, and 1.3 μL of PCR-grade water in each tube. After a brief vortex and centrifugation, the tubes were immediately placed on the Peltier Thermal Cycler (PTC-200; BIO-RAD) to perform sequence-specific reverse transcription by running 15 min at 50 °C followed by 2 min at 95 °C. Subsequently, in the same tube, the cDNA was subjected to 20 rounds of 10 s at 95 °C and 4 min at 60 °C to complete the STA reaction. For removing unincorporated primers, 3.6 μL of an Exo I Reaction solution (0.36 μL of Exonuclease I Reaction Buffer, New England Biolabs; 0.72 μL of Exonuclease I at 20 units μL^{-1}, New England Biolabs; 2.52 μL of PCR-grade water) was added to 9 μL each of STA products. After a thorough mixing, the tubes were place on the Peltier Thermal Cycler again and run for 30 min at 37 °C followed by 15 min at 80 °C.

High-throughput single-cell qPCR

The preamplified single-cell samples were diluted 5-fold prior to analysis with the Taqman Gene Expression Master Mix (Applied Biosystems) and EvaGreen DNA binding dye (Biotium), using the 48.48 Dynamic Arrays on a BioMark HD System (Fluidigm). Nested-PCR primer pairs were designed on the basis of the online Primer3 software. Amplification products of qPCR were designed to be a minimum of 2 bp shorter than the preamplified products (Table S2). All primers were synthesized by Eurofins Genomics. Ct values were calculated from the system software (BioMark Real-Time PCR Analysis; Fluidigm). A preamplified universal mouse cDNA sample was prepared as the positive control, a preamplified PCR-grade water sample was used for the no-template control. After qPCR, a comparison of the melting curves from the positive control and the experimental cells was performed to identify nonspecific signals. The relative expression of each gene (Log_2 Ex) was calculated by using the following equation:

$$\mathrm{Log}_2 E_x = 24 - \left(C_t(\text{target gene}) - C_t(Actb)\right) \quad (2)$$

Cells with absent *Actb* expression were removed from analysis (15/46, 32%). These samples were defined as no expression (No Call, NC), since all the other genes showed the efficiency of single-cell collection by FACS. The array contained 48 key genes involved in the regulation of stem cell differentiation and glucose metabolism, and three housekeeping genes (*Actb*, *Gapdh*, and *Tbp*). Statistical analysis including One-way ANOVA, hierarchical clustering (HC) and principal

component analysis (PCA) of expression data was done with SINGuLAR Analysis Toolset built on R (Fluidigm).

3. Results

Separation and re-aggregation of Flk-1(+) cells from spontaneously differentiating EBs

To optimize the timing for cell sorting, the Flk-1 expression levels induced at different days of EB culture were tested by FACS analysis. As a result, the percentage of Flk-1(+) cells increased from 3.5% ± 1.5% on day 3 to 14.9% ± 2.7% on day 8, and then decreased to 6.87% ± 0.6% on day 12 (Fig. 1A). A previous study has reported dramatic shifts in *Flk-1* gene expression as a function of differentiation dates.[18] Our result showed a high degree of similarity in this tendency on Flk-1 protein level. Fig. 1B shows the micrographs of cell masses derived from Day 3 to Day 6 Flk-1(+) cells, with an identical initial cell number (1000 cells) and cultured in 96-well U-bottom plates for further 4 days after the sorting. Interestingly, the size of cell aggregates decreased with the increase of cultivation dates before cell sorting, and aggregates could no longer form for the Flk-1(+) cells sorted on day 6 or later. The result indicates that the time point of Flk-1 protein synthesis in mesodermal progenitor cells is important when cultured them as 3D structures.

To prove the effect accurately, we separated Flk-1(+) cells generated at a late time point from those generated at earlier time point according to the literature.[7] Fig. S1 shows the procedure of FACS and re-aggregation of the four different cell groups. On day 3.25 of EB culture, cells that expressed Flk-1 protein (Day 3.25 Flk-1(+)) were defined as the early stage Flk-1(+) cells. On the other hand, Day 3.25 Flk-1(-) cells were sorted into a polydimethylsiloxane (PDMS)-coated petri dish and cultured to enable the continued differentiation. After 24h of cultivation, cells derived from Day 3.25 Flk-1(-) cells were analyzed by FACS again. At this time point, Flk-1(+) cells expressed Flk-1 protein between day 3.25 and day 4.25 (Day 3.25-4.25 Flk-1(+)) were defined as the late stage Flk-1(+) cells. The percentage of Flk-1(+) cells was related to the passage number of ESC and was within the range of 2–10% and 10–40% on day 3.25 and day 4.25, respectively. Finally, the four different cell groups (Day 3.25 Flk-1(-), Day 3.25 Flk-1(+), Day 3.25-4.25 Flk-1(+), and Day 4.25 Flk-1(-)) were collected in 96-well U-bottom plates at 1000 cells per well and allowed to culture for 10 days.

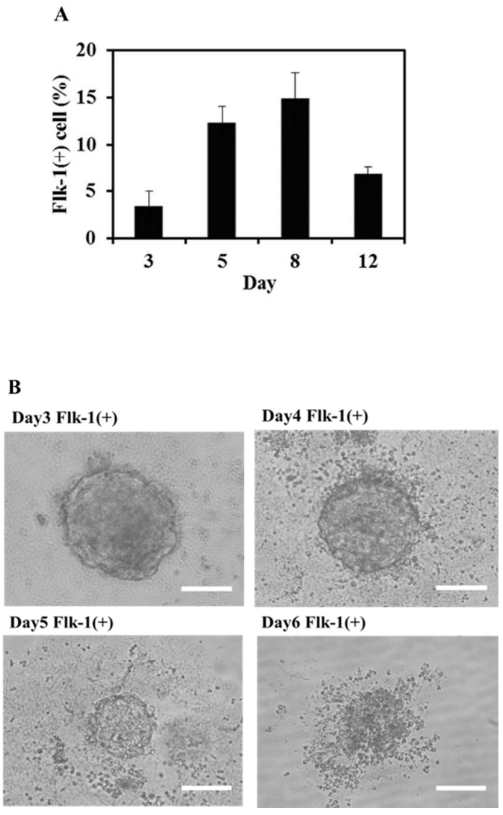

Fig. 1 (A) Percentage of Flk-1(+) cells at different dates of EB culture. (B) Micrographs of cell aggregates derived from Day 3 to Day 6 Flk-1(+) cells at day 4 after sorting. Scale bars, 200 μm.

Fig. 2A shows the average radius of cell aggregates as a function of cultivation date after the sorting. For all four cell groups, formation of cell aggregates was observed on day 1. During an additional 9 days of cultivation, cell aggregates derived from Day 3.25 Flk-1(+), Day 3.25 Flk-1(-) and Day 4.25 Flk-1(-) cells continuously grew and finally get larger than 200 μm on day 10. Interestingly, the size of cell aggregates derived from the Day 3.25-4.25 Flk-1(+) cells was kept within 150 μm during the same cultivation period. This result reflected that proliferation inhibition had specifically occurred in late stage Flk-1(+) cells when cultured them as 3D structures.

Fig. 2B shows the average OCR level per unit volume of aggregates formed on day 1 after the sorting. OCR levels of cell aggregates derived from Flk-1(+) cells tended to be smaller than those derived from Flk-1(-) cells for both sorting time points of day 3.25 and day 4.25. The lower OCR level of Flk-1(+) cells suggested that a metabolic suppression may occurred in mesodermal progenitor cells. To prove the assumption, we performed single-cell comprehensive gene expression analysis on Flk-1(+) and Flk-1(-) cell groups.

Single-cell Gene expression profiles of Flk-1(-) and Flk-1(+)

Twenty-three samples of Day 3.25-4.25 Flk-1(+) single cells and twenty-three samples of Day 4.25 Flk-1(-) single cells were

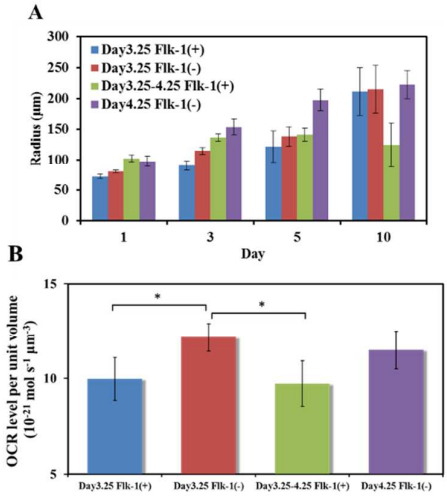

Fig. 2 (A) The average radius of cell aggregates as a function of cultivation date after the sorting (n = 5). (B) The average OCR level per unit volume of aggregates formed on day 1 after the sorting (n = 5).

collected by FACS and introduced to BioMark HD System for comprehensive gene expression analysis. Table S3 shows the comparison of average gene expression levels in the Flk-1(+) and Flk-1(-) cells. Overall, statistical analysis showed that expression levels of eight genes had significant difference between the two cell groups ($P < 0.05$). The Flk-1(+) cells showed upregulation of differentiation markers including *Kdr*, *Etv2*, *Gata2*, *Sox7* and *Gata2* and downregulation of two pluripotency markers (*Nanog* and *Pou5f1*) relative to the Flk-1(-) cells. Furthermore, we observed that there were almost no differences in expression levels of glucose metabolism markers between the two cell groups, except for *Pgm2*.

We further performed HC analysis to confirm if subgroups of single cells with different gene expression profiles were formed in Flk-1(+) or Flk-1(-) cell groups. Although there were only two cell groups (Flk-1(+) and Flk-1(-)) according to our sorting procedure, all single cell samples were mainly categorized into three separate clusters based on gene expression profiles (Fig. 3A). Interestingly, we observed that a cell cluster including two Flk-1(+) cells and four Flk-1(-) cells (marked with an asterisk in Fig. 3A) highly enriched in mesoderm markers such as *Kdr*, *Gata4*, and *Runx1*, suggesting the heterogeneity of Flk-1(-) cell group. Then we used PCA to identify the key genes that determine the expression profiles for each cell group.[19] Here, the data points are cells, each of the PC1 and PC2 components has contributions from 43-dimensional space (43 genes). PC scores represent the projections of the cell's spatial locations (gene expression patterns) onto each PC axes. PC loadings are correlation coefficients between the PC scores and the original expression patterns. Genes with the value of PC loadings close to 1 or -1 represent a high correlation to each PC axes. Fig. 3B shows scores of the first two principal components of the 31 single cell samples. Along with the PC1 axis, a cluster for Flk-1(+) cells could be distinguished from a cluster for Flk-1(-) cells. PC loading analysis of the genes contributing to the PC1 axis revealed *Nanog* and *Pou5f1* to be the most specific markers for the Flk-1(-) cell cluster, whereas *Kdr* was the most specific marker for the Flk-1(+) cell cluster (Fig. 3C). These results showed that the PC1 scores were highly correlated with the differentiation level of each cells. However, one of the Flk-1(-) cell (encircled by a dashed line in Fig. 3B) was classified into the Flk-1(+) cell cluster. We have inferred that this cell was similar to Flk-1(+) cell group in gene expression profiles but without Flk-1 protein actually being synthesized.

We next plotted the gene expression levels as a function of PC scores and used the least squares method to analyze the correlation between them. Table 1 shows the relationship between the expression levels of each gene and PC1 scores as ranked by the order of higher coefficient determination (R^2 value). Consistent with Fig. 3C, we found the PC1 scores to be positively correlated with pluripotency or ectoderm markers such as *Sox6*, *Pou5f1*, and *Syn1*, and to be inversely correlated with mesoderm or endoderm markers such as *Sox7*, *Myh7*, *Kdr*, *Pecam1*, and *Gata2*. Table 2 shows the relationship between the expression levels of each gene and PC2 scores. Among the top 10 genes showed a high degree of correlation, six genes (*Ogdh*, *Eno1*, *Aloda*, *Gpi1*, *Dld*, and *Aco2*) were related to glucose metabolism, and all of them were positively correlated with PC2 scores. On the other hand, most of the differentiation-related genes showed insignificant or weak correlations with PC2 scores. This result indicates that cells with high metabolic activity were on the far up, and cells with relatively low metabolic activity were on the far down, according to their PC2 scores in Fig. 3B.

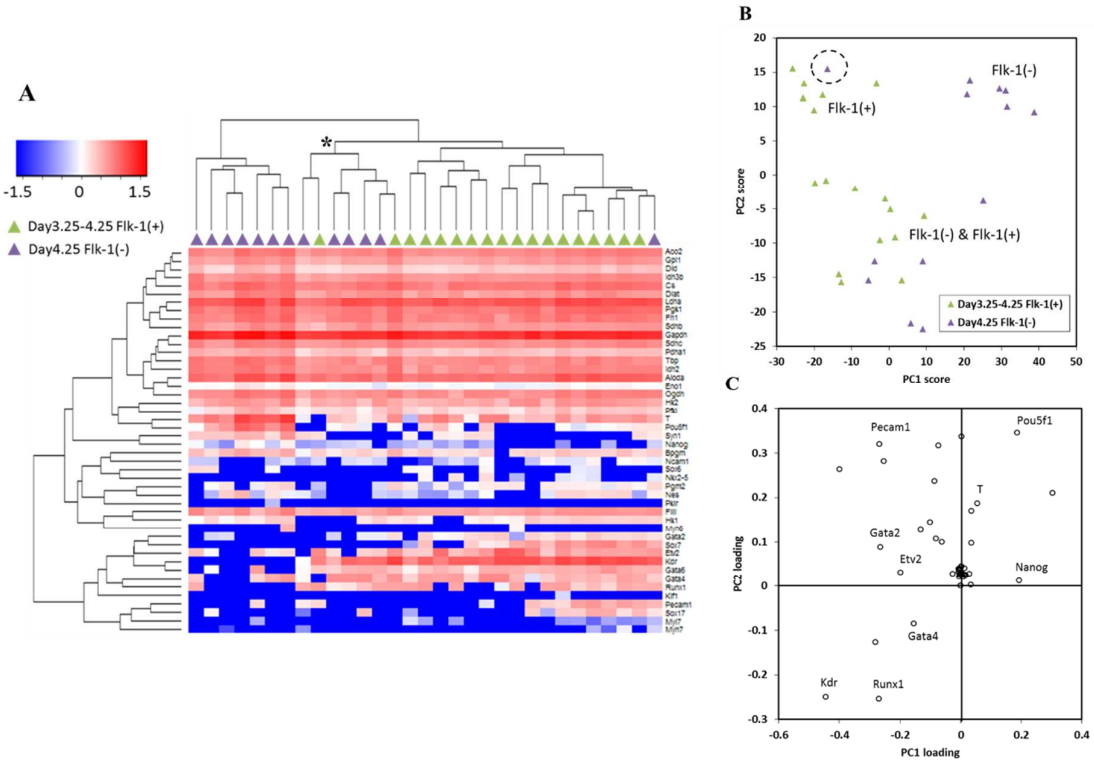

Fig. 3 (A) HC analysis of the BioMark single-cell gene expression analysis data. (B) PC scores of the 31 single cells, colored according to cell sorting of Flk-1(-) and Flk-1(+) cell groups. (C) PC loadings for each gene contribution to PC1 and PC2.

Table 1 The relationship between the expression level of each gene and PC1 scores as ranked by the order of higher coefficient determination (R^2 value).

Rank	Gene	Category	R^2	Slope
1	Sox6	mesoderm	0.7201	P
2	Sox7	endoderm	0.637	N
3	Pou5f1	pluripotency	0.6168	P
4	Syn1	ectoderm	0.5049	P
5	Myh7	mesoderm	0.4333	N
6	Kdr	mesoderm	0.4322	N
7	Pecam1	mesoderm	0.3696	N
8	Gata2	mesoderm	0.3102	N
9	Myl7	mesoderm	0.2707	P
10	Sox17	endoderm	0.2623	N
11	Gata6	endoderm	0.2586	N
12	Etv2	mesoderm	0.2584	N
13	Nanog	pluripotency	0.219	P
14	Pdha1	TCA cycle	0.1832	P
15	Tbp	house keeping	0.1692	P
16	T	mesoderm	0.1391	P
17	Hk1	glycolysis	0.1183	N
18	Ncam1	ectoderm	0.1076	N
19	Eno1	glycolysis	0.102	P
20	Bpgm	glycolysis	0.0733	P
21	Gapdh	house keeping	0.072	P
22	Sdhc	TCA cycle	0.0431	P
23	Dlat	TCA cycle	0.0429	P
24	Cs	TCA cycle	0.0244	N
25	Pgk1	glycolysis	0.0231	N
26	Idh2	TCA cycle	0.0219	P
27	Pfkl	glycolysis	0.0115	N
28	Gpi1	glycolysis	0.008	N
29	Gata4	mesoderm	0.0071	P
30	Hk2	glycolysis	0.0064	N
31	Ldha	glycolysis	0.0056	N
32	Ogdh	TCA cycle	0.0048	P
33	Pgm2	glycolysis	0.0022	P
34	Aloda	glycolysis	0.0018	P
35	Idh3b	TCA cycle	0.0018	N
36	Nes	ectoderm	0.0016	N
37	Nkx2-5	TCA cycle	0.0014	N
38	Aco2	TCA cycle	0.0014	P
39	Sdhb	TCA cycle	0.0012	P
40	Runx1	mesoderm	0.0005	N
41	Dld	TCA cycle	0.0001	P
42	Fh1	TCA cycle	0.0001	N
43	Flii	mesoderm	0.0001	N

P:positive
N:negative

Table 2 The relationship between the expression level of each gene and PC2 scores as ranked by the order of higher coefficient determination (R^2 value).

Rank	Gene	Category	R^2	Slope
1	Ogdh	TCA cycle	0.4332	P
2	Eno1	glycolysis	0.4226	P
3	Aloda	glycolysis	0.4006	P
4	Sox17	endoderm	0.3469	P
5	Gpi1	glycolysis	0.3314	P
6	Dld	TCA cycle	0.3307	P
7	Aco2	TCA cycle	0.3045	P
8	Nes	ectoderm	0.2897	P
9	Nkx2-5	mesoderm	0.2866	P
10	T	mesoderm	0.2745	P
11	Idh3b	TCA cycle	0.259	P
12	Pgk1	glycolysis	0.2577	P
13	Bpgm	glycolysis	0.2472	P
14	Hk2	glycolysis	0.2263	P
15	Fh1	TCA cycle	0.221	P
16	Idh2	TCA cycle	0.2161	P
17	Myl7	mesoderm	0.2026	N
18	Sox7	endoderm	0.1977	P
19	Kdr	mesoderm	0.1934	P
20	Hk1	glycolysis	0.1837	P
21	Syn1	ectoderm	0.1788	P
22	Gapdh	house keeping	0.1761	P
23	Tbp	house keeping	0.174	P
24	Pfkl	glycolysis	0.1708	P
25	Sdhc	TCA cycle	0.1666	P
26	Gata2	mesoderm	0.1625	P
27	Sdhb	TCA cycle	0.1572	P
28	Cs	TCA cycle	0.1568	P
29	Flii	mesoderm	0.1519	P
30	Sox6	mesoderm	0.151	N
31	Ldha	glycolysis	0.1466	P
32	Pdha1	TCA cycle	0.1335	P
33	Pgm2	glycolysis	0.1238	P
34	Pecam1	mesoderm	0.1108	P
35	Ncam1	ectoderm	0.1098	P
36	Pou5f1	pluripotency	0.104	P
37	Dlat	TCA cycle	0.0925	P
38	Myh7	mesoderm	0.0681	P
39	Runx1	mesoderm	0.0619	P
40	Gata6	endoderm	0.0505	P
41	Etv2	mesoderm	0.0422	N
42	Nanog	pluripotency	0.0333	P
43	Gata4	mesoderm	0.0191	N

P:positive
N:negative

The cluster of single-cell subgroup with low metabolic activity

As shown in Fig. 3B, a cell cluster that included both Flk-1(-) and Flk-1(+) cells (Flk-1(-) & Flk-1(+)) was separated from Flk-1(+) cell cluster and Flk-1(-) cell cluster based on PC2 scores. With the insights above, the Flk-1(-) & Flk-1(+) cell cluster could be considered as cells with low metabolic activity. To further understand the single-cell heterogeneity, we classified all of the cell samples into four subgroups on the basis of PC2 score: Flk-1(-) PC2-low (5 cells), Flk-1(-) PC2-high (7 cells), Flk-1(+) PC2-low (11 cells), and Flk-1(+) PC2-high (7 cells). For Flk-1(-) cells, there were 40% glucose metabolism-related genes (9/22) showed significant difference in average expression levels between PC2-low and PC-2 high subgroups, more than differentiation-related genes (26%, 6/23) (Fig. 4A). For Flk-1(+) cells, there were 59% glucose metabolism-related genes (13/22) showed significant difference in average expression levels between PC2-low and PC-2 high subgroups, more than differentiation-related genes (35%, 8/23) (Fig. 4B). In addition, for both Flk-1(+) and Flk-1(-) cells, PC2-high subgroups showed upregulation of glucose metabolism-related genes when compared with the PC2-low subgroups. Get together, PCA separated a subgroup with reduced metabolic activity from both the Flk-1(+) and Flk-1(-) cell groups.

Correlation between glucose metabolism-related genes and pluripotency markers at the single-cell level

We next plotted the expression levels of glucose metabolism-related genes as a function of the expression levels of differentiation-related genes to gain some insight into the mechanisms controlling metabolic activity during mesodermal differentiation. Fig. 5 show the correlation of the top six correlated glucose metabolism-related genes (*Ogdh*, *Eno1*, *Aloda*, *Gpi1*, *Dld*, and *Aco2,* according to Table 2) as a function of the expression of *Pou5f1*, a key pluripotency marker which play an important role in maintaining stemness of ECSs. For the Flk-1(+) cells, all of the six glucose metabolism-related genes indicated significant negative correlations with *Pou5f1*, as expected. In contrast, the correlation of expression levels is reversed in Flk-1(-) cells. This result that shows glucose metabolism-related genes were at their lowest expression level with the intermediate value of *Pou5f1* expression level, which represented as a U-shaped relationship in the plotting data. Expression levels of another pluripotency marker *Nanog* also showed the same U-shaped correction with expression levels of glucose metabolism-related genes, as a same manner for *Pou5f1* (Fig. S2). Furthermore, we found that almost all of the differentiation-related genes show positive correlation with glucose metabolism-related genes in expression levels for both Flk-1(+) and Flk-1(-) cells (Fig. S3-S5). Taken together, this result suggests that an intermediate differentiation state with metabolic suppression is present during mesodermal differentiation of ESCs.

4. Discussion

It has been reported that the differentiation potential of mesodermal progenitor cells meaningfully differs depending on the time point of Flk-1 protein expression, whereas other functions of the Flk-1(+) cells such as proliferation and metabolic activity remain unknown. Four cell groups including Flk-1(+) and Flk-1(-) cells in two differentiation time points were sorted and re-aggregated to form 3D structures. Among the four cell groups, only cell aggregates derived from the late stage Flk-1(+) cells (Day 3.25-4.25 Flk-1(+)) showed the reduction in proliferation potential and OCR level. In Flk-1(-) cell group, a subgroup of undifferentiated cells still exist and showed an accumulation of pluripotent markers in comparison with Flk-1(+) cell group.[20] On the other hand, although the late stage Flk-1(+) cells are currently being applied to obtain high-quality heart-contributing cells and their tissue model, after the first 24 h of re-aggregation, Flk-1(+) cells had not matured adequately, at least as far as metabolic activity is concerned. We considered this as the probable cause for the decrease in proliferation and OCR level of cell aggregates derived from the late stage Flk-1(+) cell group.

Furthermore, we compared the gene expression profiles of Day 3.25-4.25 Flk-1(+) cell group with Day 4.25 Flk-1(-) cell group at the single-cell level. By now, although a few reports have investigated the gene expression profiles in

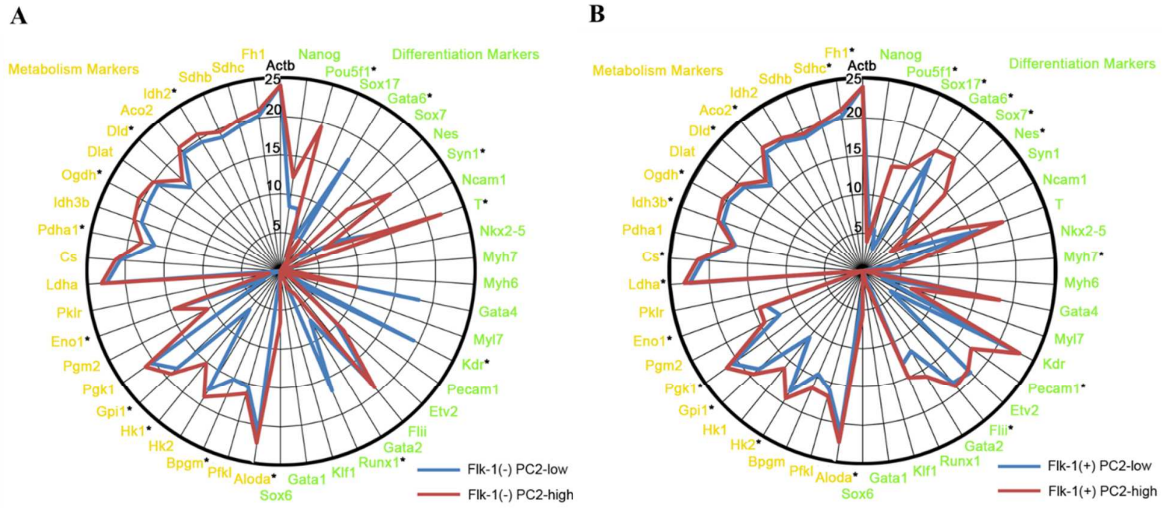

Fig. 4 The average gene expression level of 46 genes from (A) Flk-1(-) PC2-low (5 cells), Flk-1(-) PC2-high (7 cells) and (B) Flk-1(+) PC2-low (11 cells) and Flk-1(+) PC2-high (7 cells) were plotted on a radar graph. Genes with an asterisk (*) indicate a significant difference ($P < 0.05$) between the two subgroups, as determined by one-way ANOVA.

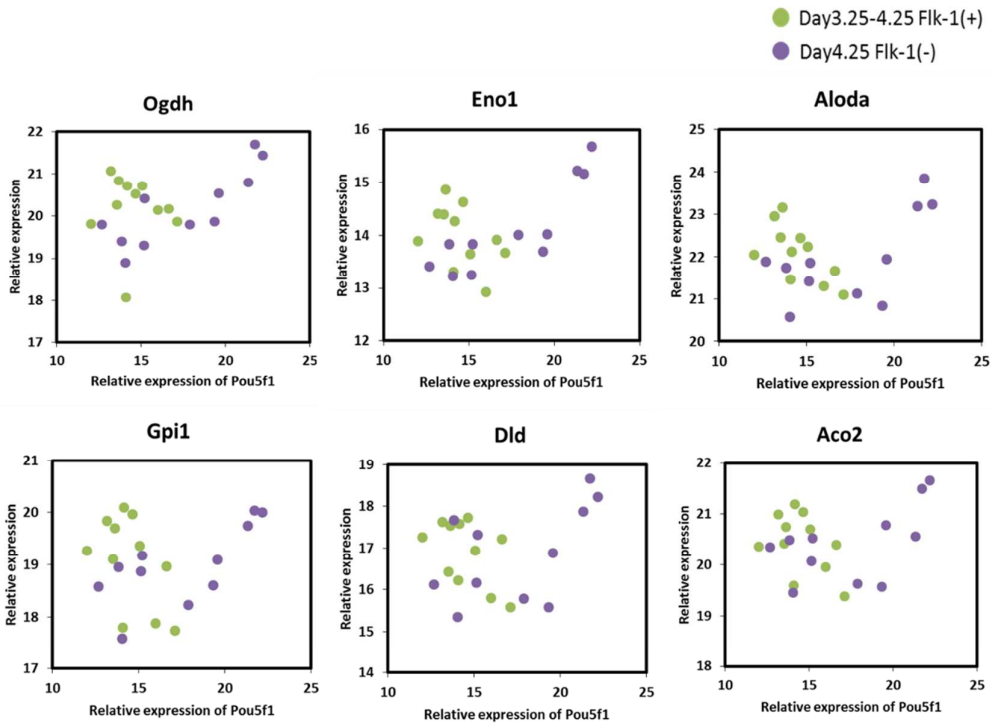

Fig. 5 The correlation of the top six correlated glucose metabolism-related genes (*Ogdh*, *Eno1*, *Aloda*, *Gpi1*, *Dld*, and *Aco2*, according to Table 2) as a function of the expression of *Pou5f1*.

undifferentiated cells and their differentiated counterparts like fibroblasts or cardiomyocytes,[9, 21] a comprehensive analysis of single mesodermal progenitor cells has not yet been studied. We found both Flk-1(+) and Flk-1(-) cells could be separated into subgroups with low/high metabolic activity on the basis of the expression levels of glucose metabolism-related genes.

It has been reported that hypoxia enhances mesodermal differentiation of both mouse and human ESCs.[10, 22] It is inferred that this effect is due to the activation of hypoxia inducible factor (HIF), which can interact with transcription factors crucial for cell differentiation.[23, 24] On the other hand, hypoxia also affects cellular metabolism directly by lowering the activity of the electron transport chain. [25] It remains unknown that if the metabolic suppression is actually needed for the generation of mesodermal progenitor cells. In the present study, we found the metabolic suppression occurring in cells expressing an intermediate level of both *Nanog* and *Pou5f1*. Because oxygen concentration was not disturbed, the metabolic suppression we observed should be an intrinsic signal occurring during mesodermal differentiation. We think our findings is applicable in relation to both mouse and human ESC sources but however, future studies will be needed to explicitly examine if similar gene expression changes also occurs *in vivo*.

Conclusions

We analyzed the metabolic features of Flk-1(+) mesodermal progenitor cells derived from mouse ESCs in detail. Cell aggregates derived from the late stage Flk-1(+) cells were shown to have a lower growth potential and OCR level than those derived from Flk-1(-) cells. We succeeded in separating subgroups with low and high metabolic activity from both Day 3.25-4.25 Flk-1(+) and Day 4.25 Flk-1(-) cells, based on single cell gene expression profiles. Our data suggested the temporary metabolic suppression is an intrinsic feature of mesodermal differentiation of ESC.

Acknowledgements

This research was partly supported by the Cabinet Office, Government of Japan, through its "Funding Program for Next Generation World-Leading Researchers" (to HS), and by the Technology for Advanced Measurement and Analysis from the Japan Science and Technology Agency (JST).

References

1. P. Van Vliet, S. M. Wu, S. Zaffran and M. Puceat, *Cardiovascular research*, 2012, **96**, 352-362.
2. J. C. Garbern and R. T. Lee, *Cell Stem Cell*, 2013, **12**, 689-698.
3. V. Kouskoff, G. Lacaud, S. Schwantz, H. J. Fehling and G. Keller, *Proceedings of the National Academy of Sciences of the United States of America*, 2005, **102**, 13170-13175.
4. J. K. Yamashita, M. Takano, M. Hiraoka-Kanie, C. Shimazu, Y. Peishi, K. Yanagi, A. Nakano, E. Inoue, F. Kita and S. Nishikawa, *FASEB journal : official publication of the Federation of American Societies for Experimental Biology*, 2005, **19**, 1534-1536.
5. L. Yang, M. H. Soonpaa, E. D. Adler, T. K. Roepke, S. J. Kattman, M. Kennedy, E. Henckaerts, K. Bonham, G. W. Abbott, R. M. Linden, L. J. Field and G. M. Keller, *Nature*, 2008, **453**, 524-528.
6. S. J. Kattman, E. D. Adler and G. M. Keller, *Trends in Cardiovascular Medicine*, 2007, **17**, 240-246.
7. S. J. Kattman, T. L. Huber and G. M. Keller, *Developmental Cell*, 2006, **11**, 723-732.

8. H. Zhang, J. L. Nieves, S. T. Fraser, J. Isern, P. Douvaras, D. Papatsenko, S. L. D'Souza, I. R. Lemischka, M. A. Dyer and M. H. Baron, *Stem cells (Dayton, Ohio)*, 2014, **32**, 191-203.
9. S. Varum, A. S. Rodrigues, M. B. Moura, O. Momcilovic, C. A. Easley IV, J. Ramalho-Santos, B. Van Houten and G. Schatten, *PloS one*, 2011, **6**, e20914.
10. D. L. Ramirez-Bergeron, A. Runge, K. D. Dahl, H. J. Fehling, G. Keller and M. C. Simon, *Development*, 2004, **131**, 4623-4634.
11. S. Bae, Y. Xiao, G. Li, C. A. Casiano and L. Zhang, *American journal of physiology. Heart and circulatory physiology*, 2003, **285**, H983-990.
12. C. Bianco, C. Cotten, E. Lonardo, L. Strizzi, C. Baraty, M. Mancino, M. Gonzales, K. Watanabe, T. Nagaoka, C. Berry, A. E. Arai, G. Minchiotti and D. S. Salomon, *The American journal of pathology*, 2009, **175**, 2146-2158.
13. S. Chung, P. P. Dzeja, R. S. Faustino, C. Perez-Terzic, A. Behfar and A. Terzic, *Nature clinical practice. Cardiovascular medicine*, 2007, **4 Suppl 1**, S60-67.
14. S. Tohyama, F. Hattori, M. Sano, T. Hishiki, Y. Nagahata, T. Matsuura, H. Hashimoto, T. Suzuki, H. Yamashita, Y. Satoh, T. Egashira, T. Seki, N. Muraoka, H. Yamakawa, Y. Ohgino, T. Tanaka, M. Yoichi, S. Yuasa, M. Murata, M. Suematsu and K. Fukuda, *Cell Stem Cell*, 2013, **12**, 127-137.
15. H. Shiku, T. Arai, Y. Zhou, N. Aoki, T. Nishijo, Y. Horiguchi, K. Ino and T. Matsue, *Molecular Biosystems*, 2013, **9**, 2701-2711.
16. Y. Zhou, T. Arai, Y. Horiguchi, K. Ino, T. Matsue and H. Shiku, *Analytical biochemistry*, 2013, **439**, 187-193.
17. H. Shiku, T. Shiraishi, S. Aoyagi, Y. Utsumi, M. Matsudaira, H. Abe, H. Hoshi, S. Kasai, H. Ohya and T. Matsue, *Analytica Chimica Acta*, 2004, **522**, 51-58.
18. T. J. Nelson, A. Chiriac, R. S. Faustino, R. J. Crespo-Diaz, A. Behfar and A. Terzic, *Differentiation*, 2009, **77**, 248-255.
19. M. Ringner, *Nat Biotech*, 2008, **26**, 303-304.
20. C. Mauritz, A. Martens, S. V. Rojas, T. Schnick, C. Rathert, N. Schecker, S. Menke, S. Glage, R. Zweigerdt, A. Haverich, U. Martin and I. Kutschka, *European Heart Journal*, 2011, **32**, 2634-2641.
21. F. Cao, R. A. Wagner, K. D. Wilson, X. Xie, J.-D. Fu, M. Drukker, A. Lee, R. A. Li, S. S. Gambhir, I. L. Weissman, R. C. Robbins and J. C. Wu, *PLoS ONE*, 2008, **3**, e3474.
22. S. Prado-Lopez, A. Conesa, A. Arminan, M. Martinez-Losa, C. Escobedo-Lucea, C. Gandia, S. Tarazona, D. Melguizo, D. Blesa, D. Montaner, S. Sanz-Gonzalez, P. Sepulveda, S. Gotz, J. E. O'Connor, R. Moreno, J. Dopazo, D. J. Burks and M. Stojkovic, *Stem cells (Dayton, Ohio)*, 2010, **28**, 407-418.
23. S. W. Lee, H. K. Jeong, J. Y. Lee, J. Yang, E. J. Lee, S. Y. Kim, S. W. Youn, J. Lee, W. J. Kim, K. W. Kim, J. M. Lim, J. W. Park, Y. B. Park and H. S. Kim, *Embo Molecular Medicine*, 2012, **4**, 924-938.
24. Q. Li, P. Hakimi, X. Liu, W. M. Yu, F. Ye, H. Fujioka, S. Raza, E. Shankar, F. Q. Tang, S. L. Dunwoodie, D. Danielpour, C. L. Hoppel, D. L. Ramirez-Bergeron, C. K. Qu, R. W. Hanson and Y. C. Yang, *Journal of Biological Chemistry*, 2014, **289**, 251-263.
25. W. W. Wheaton and N. S. Chandel, *American Journal of Physiology - Cell Physiology*, 2011, **300**, C385-C393.